Immune synapse formation requires ZAP-70 recruitment by ezrin and CD43 removal by moesin

Tal Ilani,[1] Chand Khanna,[2] Ming Zhou,[3] Timothy D. Veenstra,[3] and Anthony Bretscher[1]

[1]Department of Molecular Biology and Genetics, Cornell University, Ithaca, NY 14853
[2]Comparative Oncology Program, Center for Cancer Research, National Cancer Institute, Rockville, MD 20850
[3]Laboratory of Proteomics and Analytical Technologies, SAIC-Frederick, Inc., National Cancer Institute at Frederick, Frederick, MD 21702

Immunological synapse (IS) formation involves receptor–ligand pair clustering and intracellular signaling molecule recruitment with a coincident removal of other membrane proteins away from the IS. As microfilament–membrane linkage is critical to this process, we investigated the involvement of ezrin and moesin, the two ezrin/radixin/moesin proteins expressed in T cells. We demonstrate that ezrin and moesin, which are generally believed to be functionally redundant, are differentially localized and have important and complementary functions in IS formation. Specifically, we find that ezrin directly interacts with and recruits the signaling kinase ZAP-70 to the IS. Furthermore, the activation of ezrin by phosphorylation is essential for this process. In contrast, moesin dephosphorylation and removal, along with CD43, are necessary to prepare a region of the cell cortex for IS. Thus, ezrin and moesin have distinct and critical functions in the T cell cortex during IS formation.

Introduction

The immunological synapse (IS) is a specialized junction between a T cell and an antigen-presenting cell (APC) that forms within seconds after contact between the T cell receptor (TCR) and the appropriate antigen on the APC (Bunnell et al., 2002). The mature IS is characterized by the clustering of TCR with key signaling (e.g., PKCθ and ZAP-70) and adhesion molecules at the contact site and the exclusion of other membrane proteins such as CD43, which has a bulky extracellular domain, from the synapse region. Thus, the IS provides an accessible cellular system for studying the general question of how cells organize their cell cortex and plasma membrane into distinct functional domains. In this paper, we show the differential and essential roles of ezrin/radixin/moesin (ERM) proteins during this process.

IS formation depends on reorganization of the actin cytoskeleton in T cells induced by initial TCR signaling (Dustin and Cooper, 2000; Campi et al., 2005). The normal accumulation of filamentous actin (F-actin) at the T cell–APC interface is thought to stabilize a continuous contact between the two cells, and inhibition of actin polymerization blocks immunological synapse formation (Tskvitaria-Fuller et al., 2003; Vicente-Manzanares and Sanchez-Madrid, 2004; Campi et al., 2005). The significance of cytoskeletal changes is further illustrated by the rapid activation-induced transition from a spherical T cell with abundant microvilli to a polarized cell with few microvilli but with ruffles at the contact site (Dustin and Cooper, 2000).

The ERM proteins provide a regulated linkage between the cytoskeleton and plasma membrane, especially in actin-containing cell surface structures such as microvilli and membrane ruffles (Bretscher, 1983; Bretscher et al., 2002). Human ERM proteins, which are ∼580 residues long and share ∼75% sequence identity, are classified as members of the band 4.1 superfamily, as they have an ∼300-residue N-terminal 4.1 ERM (FERM) domain (Funayama et al., 1991; Lankes and Furthmayr, 1991). The FERM domain binds to membrane-associated proteins, whereas an F-actin–binding site lies near the C terminus (Turunen et al., 1994; Yonemura et al., 1998). ERM proteins are negatively regulated by an intramolecular interaction between the FERM and C-terminal domains that masks binding sites for F-actin and at least some membrane proteins (Gary and Bretscher, 1995; Pearson et al., 2000; Bretscher et al., 2002; Li et al., 2007). The intramolecular interaction can be relieved by phosphatidylinositol 4,5-bisphosphate in conjunction with the phosphorylation of a conserved threonine in the C-terminal domain (T567 in ezrin, T564 in radixin, and T558 in moesin) to open up the molecule and unmask the F-actin and membrane-binding sites (Hirao et al., 1996; Matsui et al., 1998; Fievet et al., 2004). Recently, phosphorylation of an additional conserved threonine in the FERM domain, T235, was also suggested to reduce the intramolecular association in ezrin (Yang and Hinds, 2003).

Correspondence to Anthony Bretscher: apb5@cornell.edu

Abbreviations used in this paper: APC, antigen-presenting cell; ERM, ezrin/radixin/moesin; F-actin, filamentous actin; FERM, 4.1 ERM; IS, immunological synapse; MS, mass spectrometry; pERM, phosphorylated ERM; TCR, T cell receptor.

The online version of this article contains supplemental material.

The Journal of Cell Biology, Vol. 179, No. 4, November 19, 2007 733–746
http://www.jcb.org/cgi/doi/10.1083/jcb.200707199

The presence of a single essential ERM protein in *Drosophila melanogaster* and *Caenorhabditis elegans* suggests a single basic function for ERM proteins (Bretscher et al., 2002). In vertebrates, the three closely related ERM members emerged by gene duplication, suggesting they may perform overlapping functions (Sato et al., 1992). Antisense phosphorothioate oligonucleotide treatment to reduce all ERM expression in cultured cells indicated that they are at least partially redundant (Takeuchi et al., 1994). In addition, no substantial differences have been reported in the ability of ERM proteins to bind multiple ligands (e.g., CD43, CD44, and intercellular adhesion molecules; Yonemura et al., 1998). Thus, it is currently believed that ERM proteins perform similar, largely redundant functions. However, their very distinct tissue distributions hint at individual cell type–specific functions (Tsukita and Hieda, 1989; Berryman et al., 1993; Amieva et al., 1994).

In primary human lymphocytes, moesin and ezrin but not radixin are expressed, with moesin being the quantitatively dominant ERM protein (Shcherbina et al., 1999). In resting T cells, phosphorylated ERM proteins are localized in microvilli (Brown et al., 2003). Stimulation of T cells by chemokine or antigen induces rapid ERM dephosphorylation (Brown et al., 2003). This presumably facilitates the loss of microvilli to create a region of the plasma membrane for T cell–APC conjugate formation. In addition, exclusion of CD43 from the contact site is mediated by moesin, ezrin, or both (Serrador et al., 1998; Allenspach et al., 2001; Delon et al., 2001). CD43 is an abundant, highly glycosylated, and sialylated transmembrane protein (Cyster and Williams, 1992) that is proposed to impede synapse formation by its negative charge and large size. Thus, the interaction between CD43 and ERM proteins seems to be required for the removal of CD43 for contact formation (Allenspach et al., 2001; Delon et al., 2001). Existing work refers to moesin and ezrin function in T cells as redundant (Shaw, 2001).

In this study, we report that ezrin and moesin perform distinct and critical roles during immunological synapse formation requiring their regulation by phosphorylation and differential association with specific ligands.

Results

Differential distribution of ezrin and moesin in resting T cells and after immunological synapse formation

To study the potentially distinct roles of ezrin and moesin in T cells, we first examined their localization in Jurkat T cells. Using specific antibodies to the two ERM proteins expressed in Jurkat T cells (Fig. S1, available at http://www.jcb.org/cgi/content/full/jcb.200707199/DC1), we found that in resting T cells, ezrin was mostly cytoplasmic, whereas moesin was enriched at the cell cortex (Fig. 1 A). However, when the cells were activated for 30 min with a soluble TCR antibody, OKT3, ezrin was redistributed to the membrane cortex (Fig. 1 A). The differential distribution of ezrin and moesin in resting T cells and the redistribution of ezrin from the cytoplasm to the cell cortex upon activation was also found in primary human T cells (Fig. 1 B). Next, we determined the localization of ezrin and moesin in the mature IS using the Raji B cell line as the APC, a system that has been well studied (Niedergang et al., 1997; Das et al., 2002; Sasahara et al., 2002; Kuhne et al., 2003). Jurkat T cells were incubated for 30 min with superantigen-loaded Raji B cells, and synapse formation was verified by clustering of the TCR and by formation of F-actin–rich protrusions that establish contact with the APC (Fig. 1 C; Bunnell et al., 2002; Tskvitaria-Fuller et al., 2003). We found that ezrin was redistributed to the IS, whereas moesin was excluded from the contact site (Fig. 1 C). As Raji B cells also express ezrin, its enrichment close to the contact site could be contributed from the B cell. To circumvent this, anti-CD3/CD28–coated polystyrene beads, which mimic activated APCs (Krawczyk et al., 2000; Nirula et al., 2006), were mixed with Jurkat T cells for 15 min, which led to conjugate formation with TCR and PKCθ at the contact site (unpublished data). Ezrin and F-actin were concentrated at the contact site, whereas moesin was excluded from it (Fig. 1 D). These data demonstrate that ezrin and moesin are differentially localized in T cells and show largely complementary distribution in the mature IS.

Dynamics of ezrin and moesin during the initial stage of T cell activation

Within 30 s after T cell/APC contact formation, TCRs cluster at the IS along with PKCθ and the tyrosine kinases Lck and ZAP-70 (Bunnell et al., 2002; Campi et al., 2005). Therefore, we examined whether ezrin and moesin redistribution occurs within this time frame. Jurkat T cells were stimulated with anti-TCR for 1 min before fixation and immunostaining. Whereas ezrin is mostly cytoplasmic in resting T cells, it was recruited to regions enriched with TCR and PKCθ after 1 min of activation. Moesin, on the other hand, was excluded from these clusters (Fig. 2 A). F-actin undergoes rapid depolymerization at the contact site after cell–cell contact and polymerizes again beneath the synapse and is enriched in the T cell protrusions (Dustin and Cooper, 2000). When we looked at T cells 1 min after activation, F-actin was excluded from TCR clusters in the same way as moesin (Fig. 2 A). Quantification of clusters formed within 1 min of activation showed that ezrin and PKCθ enriched with TCR in 86 ± 6.5% and 82.3 ± 2% of the cells, respectively. In contrast, moesin was found in clusters with TCR in only 19.6 ± 2.7% of the cells (Fig. 2 B). Similar results were found when the c ells were activated by incubation with anti-CD3/CD28–coated polystyrene beads for 1 min (Fig. 2 C). These data demonstrate that the spatial changes in ezrin and moesin distribution upon T cell activation are rapid and occur along with the clustering of TCR and other signaling molecules.

Phosphoregulation of ezrin and moesin during T cell activation

As ERM protein activity can be regulated by phosphorylation of a conserved C-terminal threonine, we examined the changes in phosphorylation of the relevant threonine, T567, in ezrin and T558 in moesin during T cell activation. In resting cells, moesin is much more highly phosphorylated than ezrin (Fig. 3 A). Upon 1–3 min of activation by soluble anti-TCR antibody, moesin is substantially but not completely dephosphorylated, as reported previously (Brown et al., 2003). Moesin dephosphorylation is

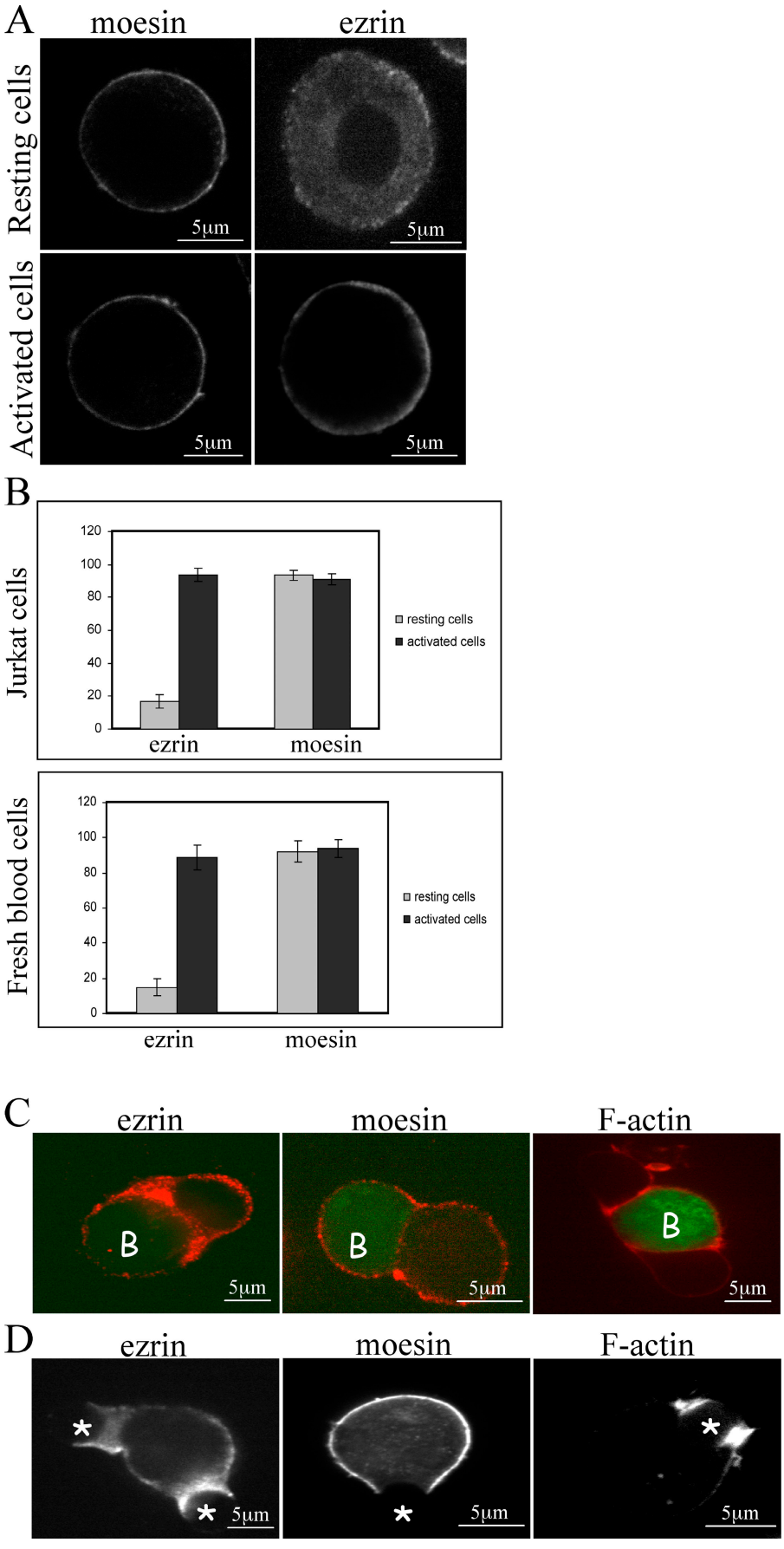

Figure 1. **Intracellular distribution of ezrin and moesin in T cells.** (A) Localization of moesin and ezrin in resting and 30-min–activated Jurkat T cells. (B) Quantitation of ezrin and moesin distribution in Jurkat and primary human T cells. The mean and SD (error bars) of three experiments examining 100 cells each is shown. (C) Jurkat T cells were incubated for 30 min with SEE superantigen–loaded B cells that were prestained with 5-chloromethylfluorescein diacetate (green; denoted by B). Cells were stained for ezrin, moesin, or F-actin (red). (D) Jurkat T cells were incubated for 15 min with anti-CD3/CD28–coated polystyrene beads and were fixed and stained (beads denoted with asterisks).

Figure 2. **Segregation of ezrin and moesin during initial T cell activation.** (A) Jurkat T cells were stimulated for 1 min with OKT3 and were fixed and stained for ezrin or moesin (green) and for CD3 actin or PKCθ (red). (B) Quantitative representation of A. The mean and SD (error bars) of three experiments examining 100 cells each is shown. (C) Jurkat T cells were incubated with anti-CD3/CD28–coated polystyrene beads for 1 min and were fixed and stained (beads denoted with asterisks).

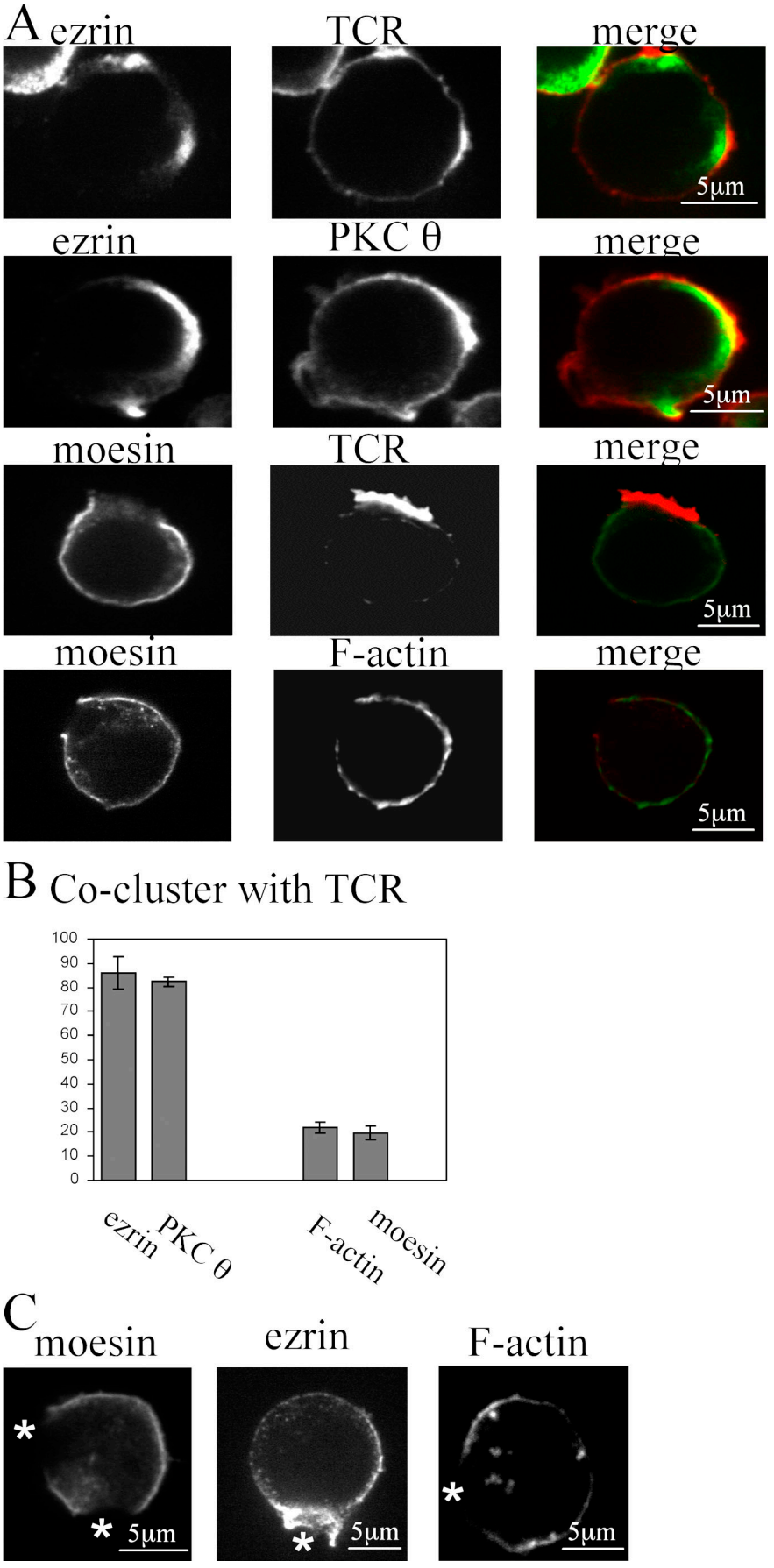

followed by phosphorylation of both ezrin and moesin after ~20 min of activation (Fig. 3 A).

When we examined the distribution of phosphorylated ERM (pERM) in the mature IS using antibody that recognizes both phosphorylated T567 ezrin and T558 moesin, it was localized both at the periphery of the synapse and at the membrane cortex outside of the contact site in conjugates between T cells and either superantigen-loaded Raji B cells or anti-CD3/CD28–coated beads (Fig. 3 B). It is known that upon chemokine stimulation of T cells, moesin is quickly and mostly dephosphorylated on T558, enabling microvilli collapse (Brown et al., 2003). When we looked at pERM at 1 min of activation, we found that similar to moesin, it was excluded from TCR clusters (Fig. 3 C). In resting T cells and after 1 min of activation, moesin is the major phosphorylated ERM protein (Fig. 3 A). Thus, pERM staining at early activation time points represents mostly the remaining phosphorylated moesin, whereas at later time points, it represents both phosphorylated ezrin and moesin that are phosphorylated on the conserved C-terminal threonine.

Phosphoregulation of ezrin and moesin is necessary for immunological synapse formation

As we found changes in the phosphorylation of ezrin and moesin during T cell activation (Fig. 3 A), we next wanted to explore their possible involvement in IS formation. To inhibit dephosphorylation, we used the phosphatase inhibitor calyculin A, which is known to inhibit ERM dephosphorylation in lymphocytes (Brown et al., 2003). 100 nM calyculin A blocked moesin dephosphorylation induced by T cell activation (Fig. S2, available at http://www.jcb.org/cgi/content/full/jcb.200707199/DC1). When Jurkat T cells were preincubated for 10 min with 100 nM calyculin A followed by 1-min activation with either anti-TCR (Fig. 3 D) or anti-CD3/CD28–coated polystyrene beads (Fig. 3 E), TCR clustering was inhibited in >90% of the cells, and, in 80% of them, no ezrin clustering was detected (Fig. 3 D). In these cells, moesin was not excluded from any cortical membrane areas, and continuous staining for pERM across the cortex membrane was seen (Fig. 3, D and E). In addition, F-actin did not depolymerize beneath any membrane segment in these cells (Fig. 3, D and E). This result suggests that moesin dephosphorylation in stimulated T cells may be required for moesin and F-actin exclusion from the contact site and for proper TCR cluster formation.

We next examined the need for the specific phosphoregulation of ezrin and moesin during IS formation. Two phosphomutants were prepared for both ezrin and moesin in which the two threonines (T235/T567 and T235/T558, respectively), which are known to be regulatory phosphorylation sites in other systems (Matsui et al., 1998; Yang and Hinds, 2003), were replaced by either alanine (ezrin-AA and moesin-AA) to preclude phosphorylation or glutamic acid residues (ezrin-EE and moesin-EE) to mimic phosphorylation. We analyzed the effects of expression of these proteins on clusters and synapse formation in Jurkat T cells. As both N- and C-terminal tagging of wild-type moesin and ezrin led to mislocalization in resting T cells (unpublished data), we used untagged proteins and verified enhanced protein expression by Western blotting (Fig. S3 A, available at http://www.jcb.org/cgi/content/full/jcb.200707199/DC1). When T cells expressing ezrin-AA were activated for 15 min with anti-CD3/CD28–coated polystyrene beads, only 7% of the cells formed a mature contact with T cell protrusions around the bead (Fig. 4, A and B). In contrast, 83% of wild-type ezrin-expressing cells formed a mature contact with activating beads after 15 min of activation (Fig. 4, A and B). Ezrin-EE was localized to the membrane cortex in resting T cells (Fig. S3 B), as it presumably represents a constitutively active form, thereby precluding an analysis of its redistribution upon stimulation. When moesin-AA was overexpressed in T cells followed by 1-min activation with anti-TCR, only 50% of the cells had TCR clusters, and it was difficult to determine whether moesin is excluded from those clusters, as overexpressed moesin-AA was highly enriched in the cytoplasm (Fig. 4, C and D). However, overexpressed moesin-EE was localized at the T cell cortex, and when the cells were activated for 1 min with anti-TCR, it was not removed from any portion of the membrane, and TCR clusters were not detected in 95% of the cells (Fig. 4, C and D). Together, these results suggest that the rapid dephosphorylation of moesin and, later, the phosphorylation of ezrin are necessary for IS formation. The differential distribution of ezrin and moesin and their phosphoregulation during T cell stimulation and IS formation were reproduced in primary human T cells (Fig. S4).

Phosphorylation of ezrin is necessary for calcium mobilization during T cell activation

After the finding that ezrin-AA prevents IS formation, we set out to explore where the signaling pathway is compromised. Elevation in cytoplasmic calcium is one of the earliest events after T cells activation (Bunnell et al., 2002; Campi et al., 2005; Yokosuka et al., 2005), so we examined changes in cytoplasmic calcium in T cells expressing ezrin and moesin phosphomutants. Calcium levels were monitored continuously for 270 s after activation using the cytoplasmic dye Fluo-LOJO. When T cells expressing wild-type ezrin or moesin were activated with anti-TCR, elevated calcium levels were recorded in 89% and 82% of the cells, respectively (Fig. 5, A and B). However, in cells expressing ezrin-AA, cytoplasmic calcium elevation was detected in only 18% of the cells. In contrast, calcium increase was detected in 72% of moesin-AA–expressing cells (Fig. 5, A and B). These data demonstrate that although ezrin is phosphorylated at later stages of synapse formation, ezrin-AA inhibits cytoplasmic calcium elevation, an early event during synapse formation. Ezrin-EE and moesin-EE, both of which localized at the cell cortex, inhibited calcium elevation to a similar extant (Fig. 5, A and B), agreeing with our findings that these two proteins inhibit initial TCR clusters and mature synapse formation.

Binding of CD43 to moesin in T cells

Several studies have suggested that CD43 is removed from the IS by binding to ERM proteins, with some discrepancy as to which ERM member is responsible (Serrador et al., 1998; Allenspach et al., 2001; Delon et al., 2001). As we found differential roles and distribution for ezrin and moesin in IS formation, we examined which ERM protein binds CD43. CD43 was found to coimmunoprecipitate with moesin from both resting

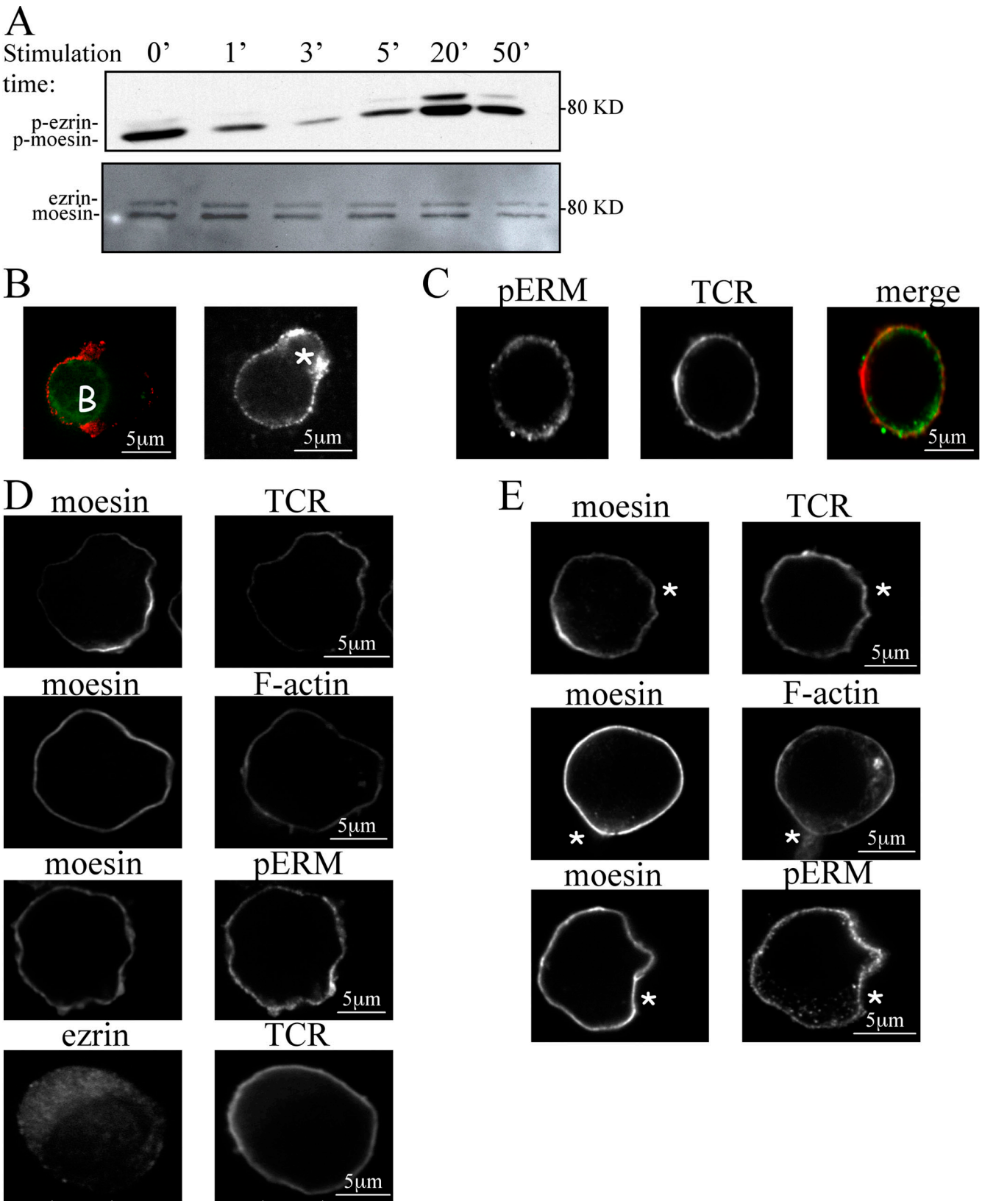

Figure 3. **Phosphoregulation of ezrin and moesin in resting T cells and in the IS.** (A) Phosphorylation level of ezrin and moesin in Jurkat T cells activated with OKT3 for various times. (B) Localization of phospho-ERM in the IS. ISs were generated between Jurkat T cells and B cells (denoted by B) or anti-CD3/CD28–coated polystyrene beads (denoted with asterisk) as described in Fig. 1 C, and cells were stained for pERM. (C) Jurkat T cells were stimulated for 1 min with OKT3 and were fixed and stained for pERM (green) and CD3 (red). (D) Calyculin A–pretreated Jurkat T cells were activated for 1 min with OKT3 and stained for the indicated proteins to examine cluster formation. (E) Calyculin A–pretreated Jurkat T cells were activated for 15 min with anti-CD3/CD28–coated polystyrene beads and stained for the indicated proteins (beads denoted with asterisks).

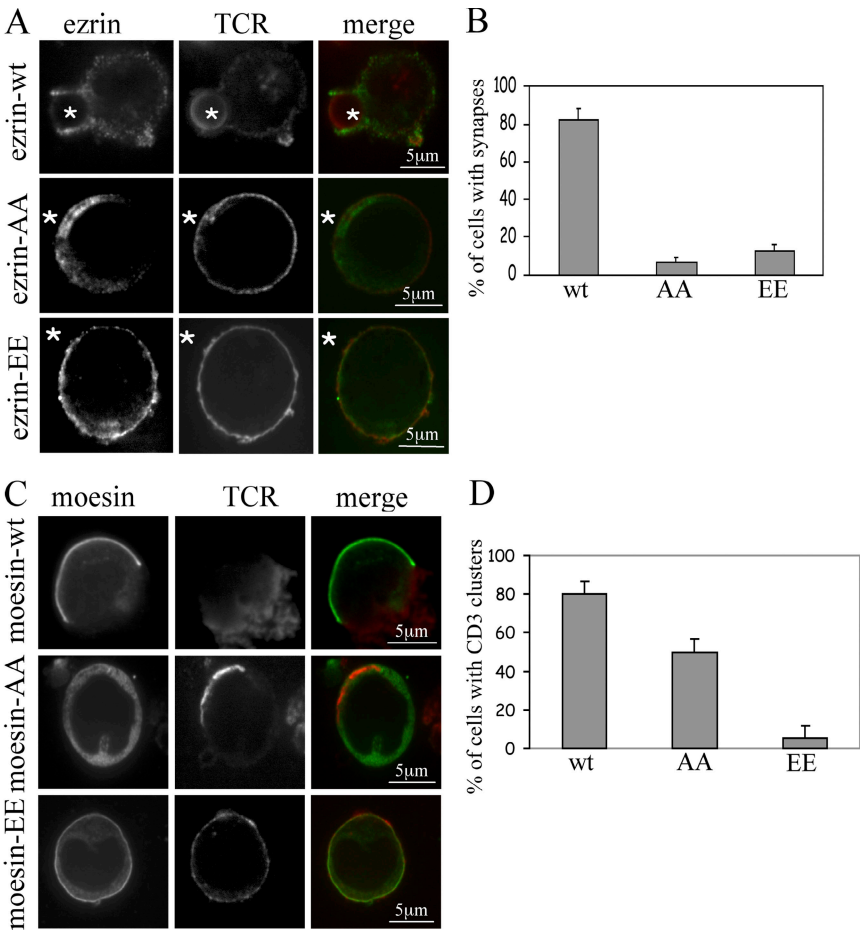

Figure 4. **Ezrin and moesin phosphomutants inhibit IS formation.** (A) Jurkat T cells overexpressing ezrin-wt, ezrin-AA, or ezrin-EE were incubated for 15 min with anti-CD3/CD28–coated polystyrene beads (denoted with asterisks) and were stained for ezrin (green) and CD3 (red). (C) Jurkat T cells overexpressing moesin-wt, moesin-AA, or moesin-EE were activated for 1 min with OKT3 and were stained for moesin (green) and CD3 (red). (B and D) Quantitative representation of A (B) and C (D). The mean and SD (error bars) of three experiments examining 70 cells each is shown.

and activated Jurkat T cells (Fig. 6 A) but not with ezrin from either resting or activated cells (Fig. 6 B). Immunofluorescence revealed colocalization of moesin with CD43 in resting and activated T cells (Fig. 6 C). This result shows that CD43 binds selectively to moesin rather than ezrin and that CD43 associated with moesin is excluded from the synapse.

Ezrin binds ZAP-70 and is necessary for its localization

As we found that CD43 binds moesin but not ezrin in T cells (Fig. 6), we sought to identify specific binding partners for ezrin. Immunoprecipitation of ezrin followed by mass spectrometry analysis was used to identify potential ezrin-binding proteins. ZAP-70, a T cell–specific Syk tyrosine kinase critical for IS formation (Chan et al., 1992; Williams et al., 1999; Campi et al., 2005), specifically coimmunoprecipitated with ezrin but not with moesin in both resting and 30-min–activated Jurkat T cells (Fig. 7 A) and, in fact, coimmunoprecipitated throughout the time course of IS formation (not depicted). ZAP-70 binds ezrin directly, as recombinant His6–ZAP-70 purified from insect cells and immobilized on nickel beads binds pure ezrin (Fig. 7 B). The binding selectivity of ZAP-70 for ezrin over moesin is potentially determined by their FERM domains, as recombinant His6–ZAP-70 preferentially binds the ezrin FERM domain (Fig. S5 C, available at http://www.jcb.org/cgi/content/full/jcb.200707199/DC1). This domain was previously shown to include the binding site for several ligands (Yonemura et al., 1998).

In resting Jurkat T cells, ZAP-70 is localized at the cell cortex (Huby et al., 1997), whereas the bulk of ezrin is cytoplasmic (Fig. 7 C). However, after 1 min of activation by soluble TCR antibody, ezrin and ZAP-70 precisely colocalize in clusters (Fig. 7 C). To decipher the apparent paradox of ezrin and ZAP-70 distributions in resting T cells, we analyzed the properties of the ZAP-70–bound fraction of ezrin in T cells. For this, ZAP-70 was quantitatively immunoprecipitated from Jurkat T cells (Fig. S5 A) together with ∼15% of total ezrin (Fig. S5 B). Thus, a small fraction of ezrin may be bound to ZAP-70 at the cortex and not readily detectable by light microscopy. By characterizing the ezrin coprecipitating with ZAP-70 with an equivalent amount of ezrin that was directly immunoprecipitated, we found that ZAP-70 preferentially binds the threonine T567-phosphorylated form of ezrin, which is known to be the activated form and, thus, is more likely to be associated with membrane-bound proteins (Fig. 7 D).

To explore the role of ezrin phosphorylation on ZAP-70 localization, its localization in Jurkat T cells expressing ezrin mutants was examined. In 88% of the cells expressing ezrin-AA, both ezrin and ZAP-70 were cytoplasmic and remained largely cytoplasmic after activation with anti-TCR (Fig. 7 E). These results suggest that ezrin-AA perturbs ZAP-70 localization at the cell cortex and prevents its clustering upon T cell stimulation.

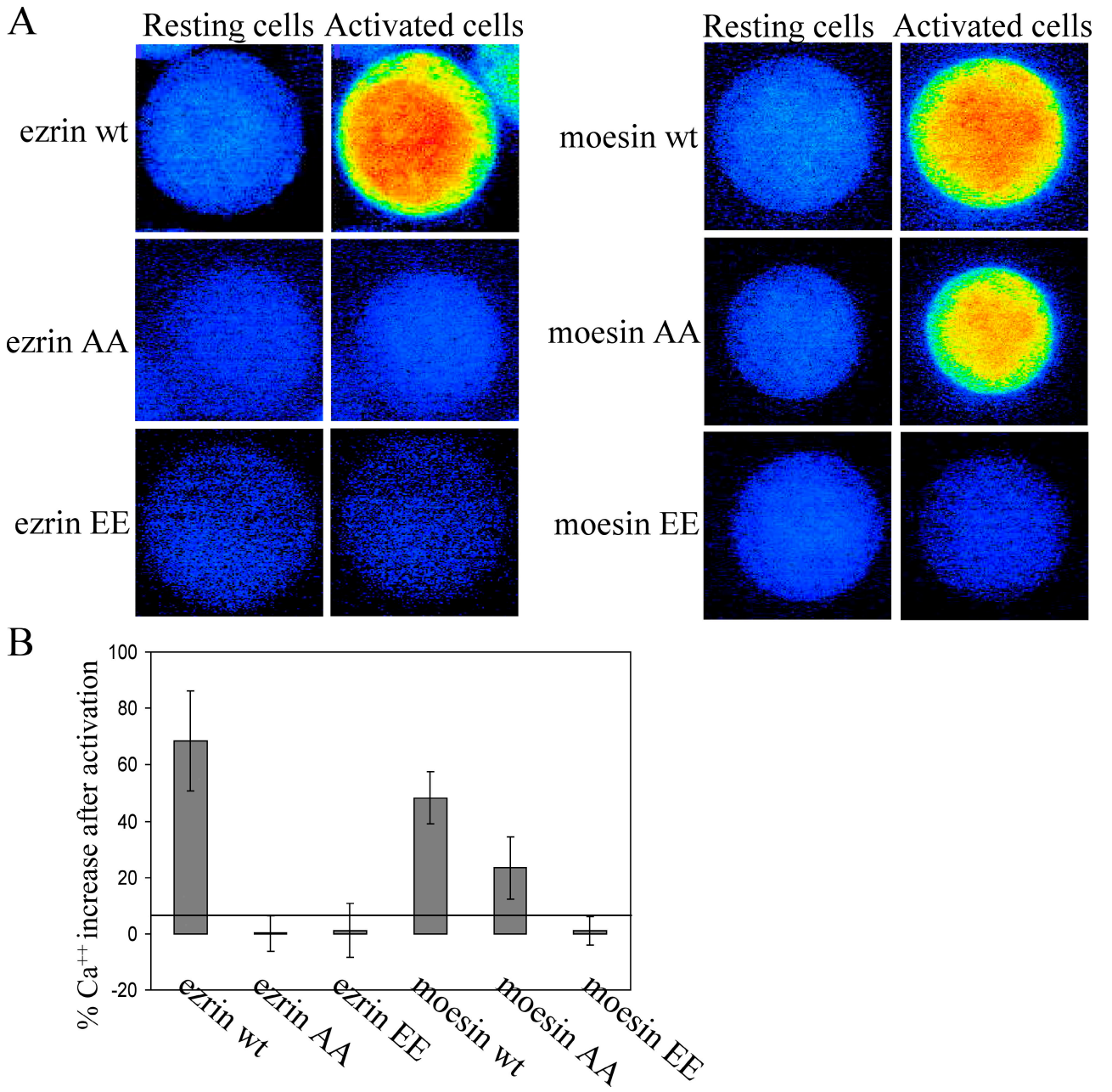

Figure 5. **Effect of ezrin and moesin phosphomutants on calcium mobilization.** (A) Jurkat T cells overexpressing various ezrin and moesin phosphomutants were incubated with the cytoplasmic calcium-sensitive dye Fluo-LOJO. Cells were analyzed before and 1 min after activation with OKT3. (B) Quantitative representation of A. The mean and SD (error bars) of three experiments examining 70 cells each is shown.

The cortical distribution of ezrin-EE did not affect ZAP-70 cortical localization but inhibited their coclustering at the cortex altogether (Fig. 7 F). Binding of ZAP-70 to the different ezrin mutants was verified by Western blot analysis (Fig. S5 D). To determine whether phosphorylation of one or both threonines is required for ZAP-70's cortical recruitment, two single-A ezrin mutants were generated and introduced into Jurkat T cells (ezrin-T235A and ezrin-T567A). Although 85% of resting cells expressing ezrin-T235A showed a wild-type distribution of ezrin and ZAP-70, 91.4% of resting cells expressing ezrin-T567A had a cytoplasmic distribution of both ezrin and ZAP-70 (Fig. 7 G). Similar results were obtained when cells were stimulated with anti-TCR; namely, ezrin- T235A expression allowed proper cluster formation, whereas both ezrin and ZAP-70 remained cytoplasmic in ezrin-T567A–expressing cells (Fig. 7 H). Collectively, these results show that threonine T567 in ezrin is critical to allow the proper localization of ZAP-70 in resting cells and for the rapid recruitment of ZAP-70 during IS formation.

ZAP-70 is mislocalized in ezrin knockdown cells

Our findings that proper ZAP-70 localization in T cells and recruitment to the IS requires phosphoregulated ezrin most likely

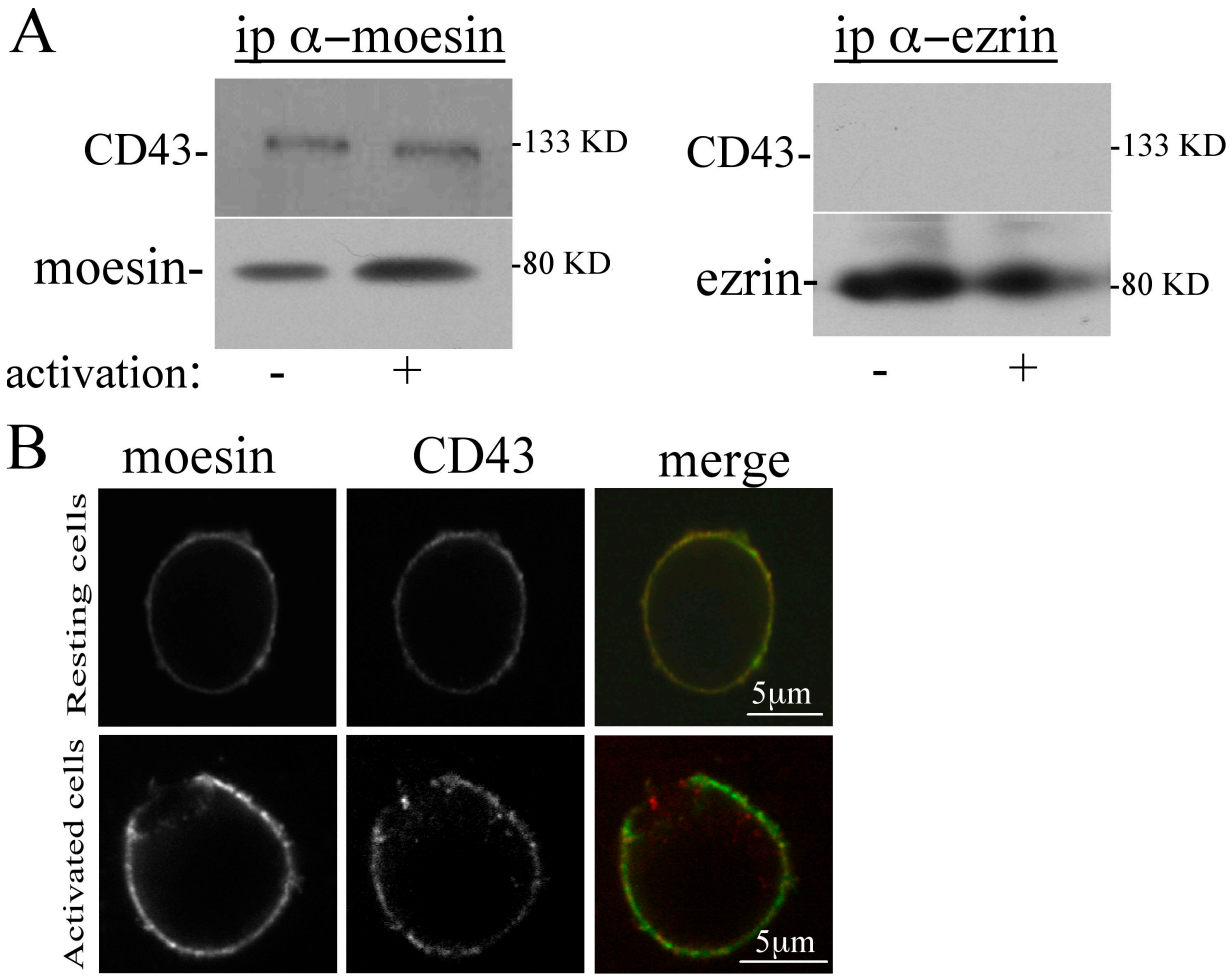

Figure 6. **CD43 specifically coimmunoprecipitates with moesin.** (A and B) Moesin (A) and ezrin (B) immunoprecipitates from resting and activated Jurkat T cells immunoblotted with CD43 and moesin or ezrin antibodies. (C) Resting and 1-min–activated Jurkat T cells were fixed and stained for moesin (green) and CD43 (red).

indicates the need for direct interaction between these two proteins. As an independent method to assess whether ezrin is necessary for ZAP-70 localization, Jurkat T cells were specifically depleted of ezrin using siRNA (Fig. 8 A). 73% of resting T cells depleted of ezrin had a cytoplasmic distribution of ZAP-70 (Fig. 8 B), which failed to cluster and remained cytoplasmic after 1 min of activation with anti-TCR (Fig. 8 C). When ezrin-depleted cells were activated for 15 min with anti-CD3/CD28–coated polystyrene beads, conjugate formation was inhibited in 84% of the cells, and ZAP-70 remained cytoplasmic (Fig. 8 D). These data further demonstrate that ZAP-70 requires ezrin for proper localization in T cells and for clustering at the IS and that moesin cannot provide this function.

Discussion

Formation of the IS involves segregation of the TCR with key signaling molecules to the T cell–APC interface and the exclusion of other specific membrane proteins. These dynamic changes are accompanied by TCR-mediated structural changes and cellular organization of the cytoskeleton. ERM proteins have been implicated in morphological changes and membrane–cytoskeletal rearrangements during synapse formation, and they are often considered to be functionally redundant. We examined the distribution and roles of the two ERM proteins expressed in T cells, ezrin and moesin, during synapse formation. Our results show that ezrin and moesin are differentially localized and, through phosphorylation-regulated processes, perform functionally distinct roles during IS formation as well as interact with different binding partners.

Functional redundancy for vertebrate ERM proteins is consistent with the findings that loss of the single ERM protein in the insect *D. melanogaster* (Speck et al., 2003) or nematode *C. elegans* (Gobel et al., 2004) is lethal, whereas gene knockouts of moesin (Doi et al., 1999) or radixin in mice are not, although radixin-deficient mice do have defects associated with liver function and hearing (Kikuchi et al., 2002; Kitajiri et al., 2004). However, ezrin knockout mice die within 2 wk of birth, possibly as a result of defects in intestinal epithelial cell morphology (Saotome et al., 2004). These differential phenotypes do not disprove functional redundancy, as ERM proteins show distinct tissue distributions, with ezrin being found highly enriched in

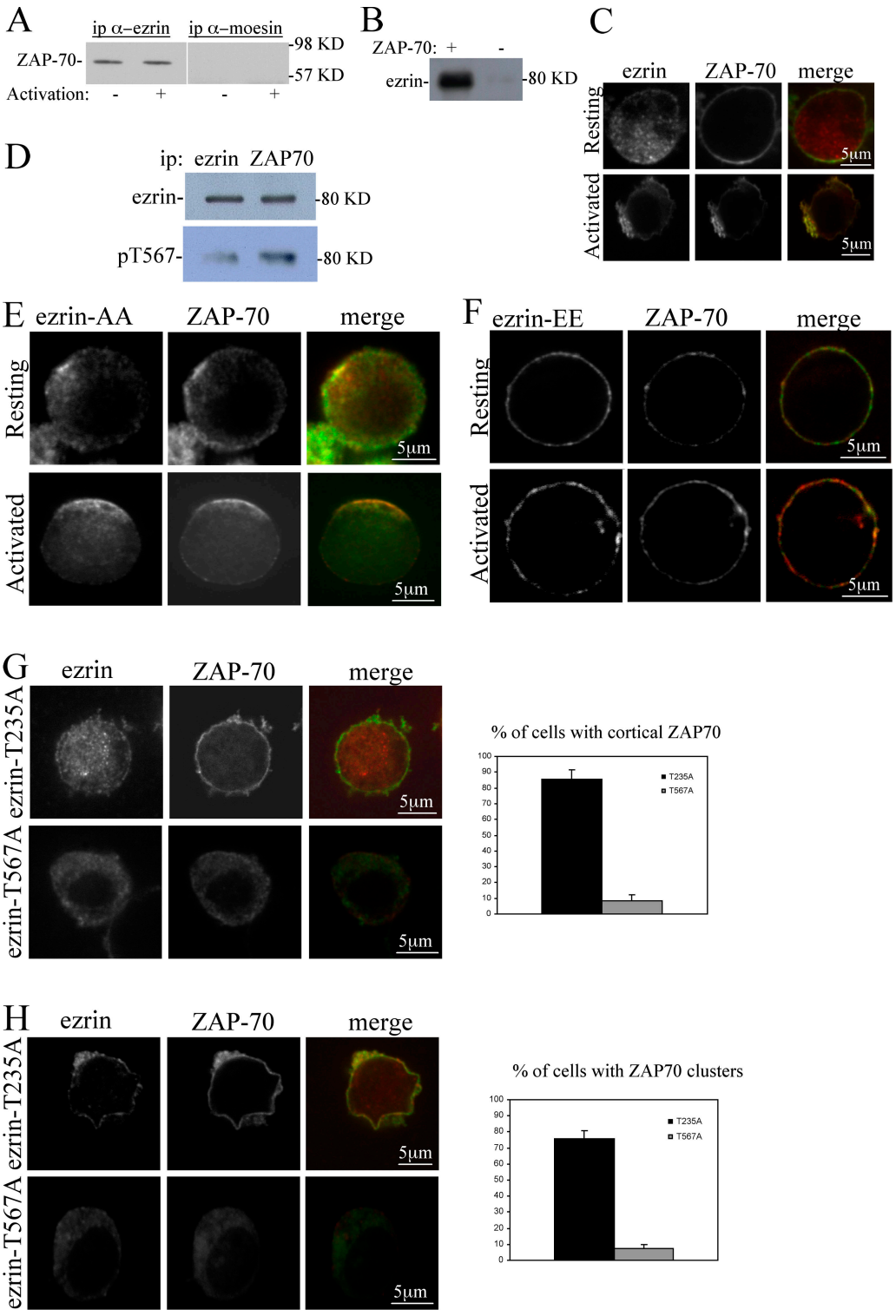

Figure 7. **Ezrin specifically interacts with ZAP-70 and is necessary for its localization at the IS.** (A) Ezrin or moesin immunoprecipitates from resting and activated Jurkat T cells immunoblotted with ZAP-70 antibodies. (B) Ezrin directly binds nickel bead–immobilized 6His–ZAP-70. (C) Resting and 1-min–activated Jurkat T cells were fixed and stained for ezrin (red) and ZAP-70 (green). (D) ZAP-70 and ezrin immunoprecipitates from resting T cells adjusted to contain the same amount of ezrin immunoblotted with ezrin or anti-pERM antibodies. (E and F) Jurkat T cells overexpressing ezrin-AA (E) or ezrin-EE (F) were activated for 1 min with OKT3 and stained for ezrin (green) and ZAP-70 (red). (G and H) Jurkat T cells overexpressing ezrin-T235A (G) or ezrin-T567A (H) were activated for 1 min with OKT3 and stained for ezrin (green) and ZAP-70 (red). On the right, quantitative representation of G and H. The mean and SD (error bars) of three experiments examining 70 cells each is shown.

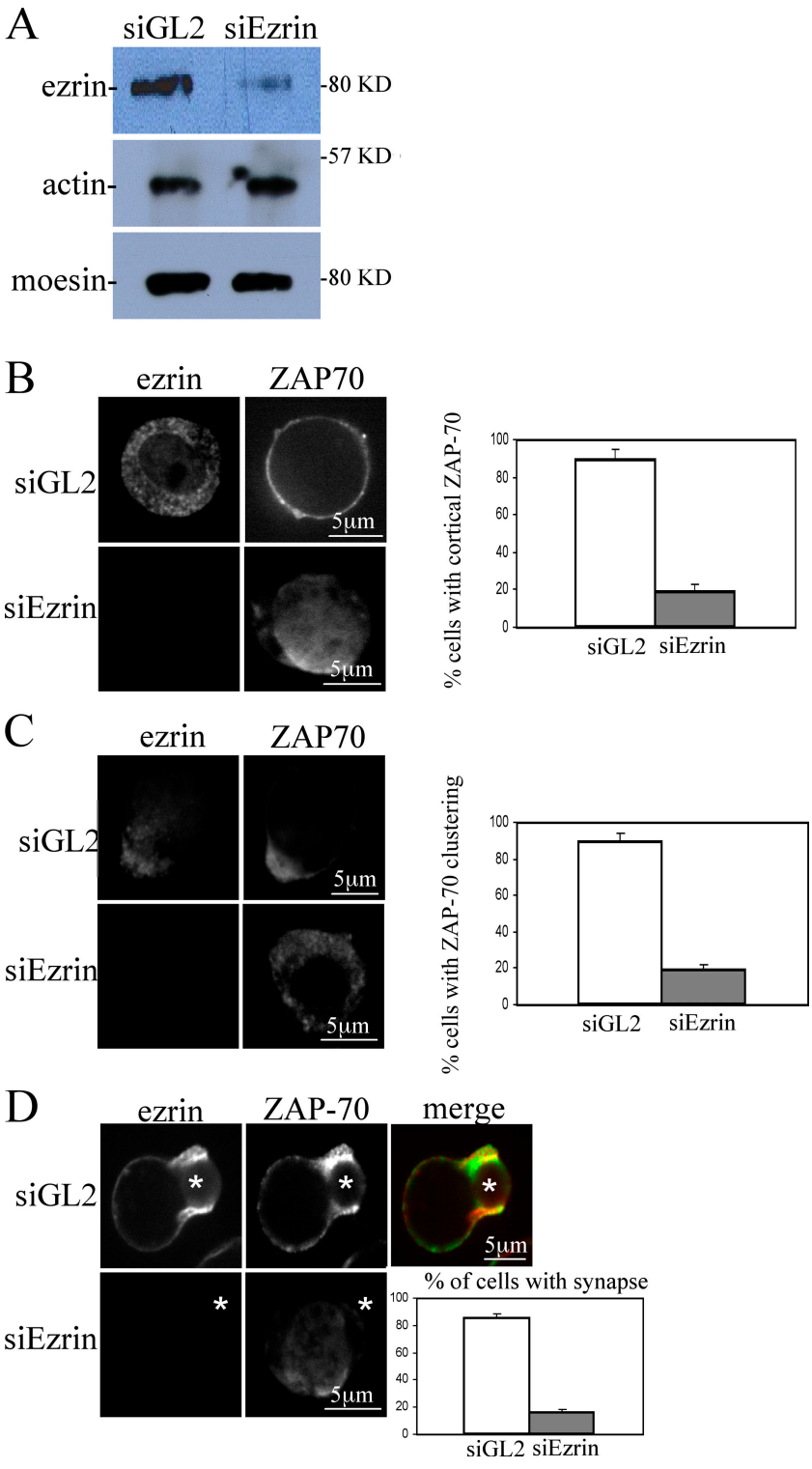

Figure 8. **ZAP-70 is mislocalized in ezrin-depleted T cells.** (A) Jurkat T cells were transfected with siRNA against ezrin or GL2 luciferase and analyzed by immunoblotting for ezrin, F-actin, and moesin expression. (B) Jurkat T cells were transfected with siRNA against ezrin or GL2 luciferase and were fixed and stained for ezrin and ZAP-70. (C) Jurkat T cells were transfected with siRNA against ezrin or GL2 luciferase, stimulated for 1 min with OKT3, and fixed and stained for ezrin and ZAP-70. (B and C) On the right, quantitative representation. (D) Jurkat T cells were transfected with siRNA against ezrin or GL2 luciferase, activated for 15 min with anti-CD3/CD28–coated polystyrene beads, and fixed and stained for ezrin and ZAP-70 (beads denoted with asterisks). The bottom right panel is a quantitative representation. (B–D) The mean and SD (error bars) of three experiments examining 100 cells each is shown.

polarized epithelial cells (Berryman et al., 1993), radixin being the dominant member in liver (Tsukita and Hieda, 1989), and moesin being enriched in endothelial cells and lymphocytes (Lankes and Furthmayr, 1991; Shcherbina et al., 1999). In support of redundancy, when each ERM was individually suppressed in cultured thymoma cells, their microvilli were not affected, but loss of all three eliminated microvilli (Takeuchi et al., 1994). However, none of these studies explored the question of whether ERM members might play distinct roles within the context of a single cell.

What functions might ezrin and moesin perform in synapse formation? During IS formation, changes in T cell shape occur, including the disappearance of microvilli and flattening of the membrane followed by actin polymerization and ruffle formation at the T cell–APC interface. We show that in resting T cells, moesin and phosphomoesin are enriched at the cell cortex.

Upon stimulation, moesin is very rapidly dephosphorylated and lost along with its ligand CD43 specifically from the contact site, and both are then absent from this region until at least 30 min after IS formation. The relevance of moesin dephosphorylation in this process is implied by the finding that treatment with the phosphatase inhibitor calyculin A inhibited both moesin dephosphorylation and its local loss during T cell activation. More specifically, expressing a mutant that mimics constitutive phosphorylation (moesin-EE) abolished the localized loss of moesin at the contact site as well as IS formation. Thus, rapid moesin dephosphorylation plays a critical role in preparing a region of the cell cortex for synapse formation.

Ezrin plays a different role. In resting T cells, the bulk of ezrin is localized to the cytoplasm in a dephosphorylated dormant state. Within 1 min of activation, ezrin becomes enriched at the contact site with TCR and key signaling molecules. At later times, ezrin is phosphorylated and colocalizes with F-actin at the immunological synapse, a region devoid of moesin. The importance of ezrin phosphorylation in this process was demonstrated by examining cells in which a nonphosphorylatable mutant (ezrin-AA) was expressed. Initial TCR clusters were formed in 50% of these cells, but mature synapse formation was almost completely abolished. This implies that delayed phosphorylation of ezrin contributes to stabilizing the spatial segregation of molecules at the contact site. Surprisingly, ezrin-AA expression also blocked the rapid calcium elevation that is seen within 30–60 s after T cell stimulation. As the inhibition of calcium mobilization was specific to ezrin-AA (and was not detected with moesin-AA), it suggested that ezrin may be involved upstream in the signaling cascade of T cells rather than merely stabilizing the mature synapse.

We have found that ezrin binds directly to ZAP-70, a T cell–specific nonreceptor tyrosine kinase that plays an integral role in TCR signaling, in resting T cells as well as throughout synapse formation. ZAP-70 is localized to the cell cortex in resting Jurkat T cells and is rapidly phosphorylated by Lck and recruited to TCR clusters upon T cell activation (Huby et al., 1997; Bunnell et al., 2002; Campi et al., 2005; Yokosuka et al., 2005). A previous study showed that ezrin and/or moesin interacts with Syk tyrosine kinase, a protein closely related to ZAP-70 (Urzainqui et al., 2002). The significance of proper recruitment of ZAP-70 to the TCR signaling complex is demonstrated in patients with common variable immunodeficiency in which ZAP-70 fails to properly localize, leading to defective T cell differentiation (Boncristiano et al., 2000), and by impaired T cell activation in various forms of the severe combined immunodeficiency disease, in which ZAP-70 was affected (Chan et al., 1994). Biochemical characterization of ZAP-70–ezrin interaction revealed that ZAP-70 preferentially binds the threonine-phosphorylated form of ezrin. This fraction of ezrin most likely represents an activated form of ezrin that can be attached to membrane-bound proteins rather than the dormant, nonphosphorylated ezrin that we found to be mostly cytoplasmic. We have also examined whether ZAP-70 could be the tyrosine kinase that phosphorylates ezrin, but our in vitro experiments did not support this possibility (unpublished data).

We found that ezrin-AA expression perturbs ZAP-70 distribution and prevents its recruitment to clusters upon activation. Expression of single-alanine mutants of ezrin (T235A or T567A) showed that phosphoregulation of only one of these two threonines, T567, is required for ZAP-70 localization in T cells and recruitment to the IS. Depletion of ezrin by specific siRNA treatment from Jurkat T cells leads to the same phenotype as expression of the ezrin-AA mutant: namely, cytoplasmic distribution of ZAP-70 and lack of clustering at the site of activation. These results demonstrate the central role of ezrin regulation in the correct targeting of ZAP-70 in the T cell.

As far as we are aware, this is the first study to show functionally distinct and phosphoregulated contributions for ezrin and moesin in a defined cellular process. Moreover, we were able to show that mutants altered in the ability to be dephosphorylated or phosphorylated revealed distinct contributions of ezrin and moesin in IS formation. In addition, we have uncovered ligands that bind selectively to ezrin and moesin. The molecular basis for the functional distinction and binding preferences between such closely related proteins is not yet resolved and suggests that fruitful approaches will be able to determine which sequences define their distinct contributions and what biochemical differences distinguish ezrin and moesin function in T cells.

Materials and methods

Cell lines and antibodies

All cells were purchased from American Type Culture Collection. Antibodies against human ezrin, moesin, and pERM have been described previously (Bretscher, 1989; Reczek et al., 1997). Rabbit anti–human ERM and mouse anti–human ZAP-70 were obtained from Cell Signaling Technology. R-phycoerythrin–labeled mouse anti–human CD3 and mouse anti–human CD43 were obtained from BD Biosciences. Mouse anti–human PKCθ was obtained from Santa Cruz Biotechnology, Inc. OKT3 mouse anti–human CD3 was purified from the OKT3 hybridoma cell line. Rhodamine phalloidin, AlexaFlour568 phalloidin, donkey anti–rabbit and donkey anti–mouse AlexaFlour488, and goat anti–rabbit and goat anti–mouse AlexaFlour568 were obtained from Invitrogen. HRP-conjugated goat anti–rabbit antibodies were obtained from MP Biomedicals.

Constructs

Human moesin-wt entry vector was generated by PCR from pQE16-moesin using the primers 5′-CCAGTGTGGTGGAATTCATGCCCAAAACGATC and 3′-AGATATCTCGAGGCTAATTAAGCTTGTTACATAGACTCAAATTCG. PCR product was ligated into TOPO TA cloning vector (Invitrogen) for sequence verification, digested using EcoRI and XhoI restriction enzymes, and ligated into pENTR 3C entry vector (Invitrogen). Human moesin-AA and moesin-EE entry vectors were generated from moesin-wt entry vector in two steps. First, T235A/E mutants were generated by PCR using the following primers: T235A (5′-GAATGACAGACTAGCACCCAAGATAGGC), T235A (3′-GCCTATCTTGGGTGCTAGTCTGTCATTC), T235E (5′-GAATGACAGACTAGAACCCAAGATAGGC), and T235E (3′-GCCTATCTTGGGTTCTAGTCTGTCATTC). PCR products and moesin-wt entry vector were digested using BglI and BglII restriction enzymes, ligated, and sequence verified. Second, AA/EE mutants were generated by PCR using the following primers: T558A (5′-GACAAATACAAGGCACTGCGCCAGATC), T558A (3′-GATCTGGCGCAGTGCCTTGTATTTGTC), T558E (5′-GACAAATACAAGGAACTGCGCCAGATC), and T558E (3′-GATCTGGCGCAGTTCCTTGTATTTGTC). PCR products and entry vectors from first step were digested using BglI and XhoI restriction enzymes, ligated, and sequence verified. All entry vectors were then exchanged into pDEST 12.2 expression vector (Invitrogen) by LR clonase reaction. Human ezrin entry and expression vectors were generated in a similar way by J.I.A. Thoms (Cornell University, Ithaca, NY). GST–ZAP-70 expression vector was provided by A.C. Chan (Genentech, Inc., South San Francisco, CA).

Immunofluorescence

T cells or cell conjugates were plated onto poly-L-lysine–coated glass slides, fixed for 30 min at RT with 3.7% formaldehyde followed by permeabilization in 0.1% Triton X-100 in PBS for 2 min, and rinsed three times in PBS. Cells were then incubated for 1 h with 5% BSA in PBS followed by incubation

with primary antibody in 5% BSA in PBS for 1 h, washed in PBS, and incubated with appropriate secondary antibody (or phalloidin) in 5% BSA in PBS for 1 h. After additional washes, 5 μl Vectashield (Vector Laboratories) was added to the cells, and slides were covered with coverslips. Cells were observed on a microscope (Eclipse TE-2000U; Nikon) with a 100× 1.4 NA lens using a spinning disk confocal imaging system (UltraView LCI; PerkinElmer) and a 12-bit digital output charge-coupled device camera (C4742-95-12ERG; Hamamatsu).

Western blotting
Jurkat and primary T cells were lysed and resolved by SDS-PAGE followed by transfer to polyvinylidene difluoride membranes (Immobilon-P; Millipore) using a semidry transfer system (Integrated Separation Systems). After 1-h blocking in 5% dry milk, TBS–Triton X-100 membranes were incubated with primary antibody for 1 h, washed, and incubated for 1 h with appropriate HRP-conjugated secondary antibody. Blots were developed using ECL (GE Healthcare).

T cell stimulation and conjugates formation
Jurkat and primary human T cells were activated with 10 μg/ml OKT3 antibody for the indicated times. For stimulation with beads, 10^7 T cells were mixed with 2×10^5 anti-CD3/CD28–coated polystyrene beads (Invitrogen) for the indicated times. For stimulation with B cells, Raji B cells were fluorescently labeled with 5-chloromethylfluorescein diacetate (CellTracker; Invitrogen) and loaded with 2 μg/ml SEE superantigen (Toxin Technology). B cells were then mixed with an equal number of T cells for the indicated times.

Transfection
Transient transfection of Jurkat T cells was performed using GenePORTER (Gene Therapy Systems) according to the manufacturer's instructions. Transfection efficiency was between 60 and 70% as determined by cotransfection with red fluorescent protein. Cells overexpressing untagged ERM mutants were easily identified by their higher fluorescent intensity compared with nontransfected cells.

Isolation of primary human T cells
Human peripheral blood lymphocytes were isolated from citrate-anticoagulated whole blood by dextran sedimentation (Blood Centers of America) followed by density separation over Ficoll-Hypaque (Sigma-Aldrich). The resulting mononuclear cells were washed in PBS and further purified by nylon wool and plastic adherence as described previously (Dustin and Springer, 1988). The resulting lymphocytes were >90% $CD3^+$ T lymphocytes as verified by FACS analysis.

Immunoprecipitation
Jurkat T cells were lysed in cold radioimmunoprecipitation assay buffer (0.1% SDS, 1% Triton X-100, 1% deoxycholate, 150 mM NaCl, 1 mM EDTA, and 25 mM Tris, pH 7.4) with protease inhibitors, and lysates were centrifuged for 10 min at 55,000 rpm at 4°C. Supernatants were mixed with either protein A–Sepharose beads (Sigma-Aldrich) precoated with antimoesin polyclonal antibodies or cyanogen bromide–activated Sepharose 4B beads (Sigma-Aldrich) precoated with antiezrin polyclonal antibodies and incubated for 2 h with constant rotating. Beads were washed six times with radioimmunoprecipitation assay buffer, and pellets were resuspended in SDS sample buffer, boiled, and resolved on 7.5% SDS-PAGE.

Calcium mobilization assay
Jurkat T cells were cotransfected with the relevant ERM construct and red fluorescent protein. 48 h after transfection, cells were plated on a poly-L-lysine–coated glass-bottom culture dish and labeled with 1 μM Fluo-LOJO (TefLabs). Cells were observed before and during activation with 10 μg/ml OKT3 antibody on an Eclipse TE-2000U microscope using the UltraView LCI spinning disk confocal imaging system.

Mass spectrometric analysis
Protein bands excised from the SDS-PAGE gel were destained before digestion with trypsin overnight at 37°C. Peptides were extracted with a solution of 70% acetonitrile and 0.1% trifluoroacetic acid and were desalted using C-18 ZipTip (Millipore). The samples were then lyophilized and resuspended in 0.1% trifluoroacetic acid before mass spectrometry (MS) analysis. Protein identification was performed by nanoflow reversed phase liquid chromatography tandem MS using a nanoflow liquid chromatography system (Agilent 1100; Agilent Technologies) coupled online with a linear ion trap MS (LTQ; ThermoElectron). Nano-reversed phase liquid chromatography columns were slurry packed in-house with 5 μm of 300-Å pore size C-18 phase (Jupiter) in a 75-μm i.d. × 10-cm fused silica capillary (Polymicro Technologies) with a flame pulled tip. After sample injection, the column was washed for 20 min with 98% mobile phase A (0.1% formic acid/water) at 0.5 μl/min, and peptides were eluted using a linear gradient of 2–42% mobile phase B (0.1% formic acid/acetonitrile) for 40 min at 0.25 μl/min and then 98% mobile phase B for 10 min. The linear ion trap MS was operated in a data-dependent mode in which each full MS scan was followed by five MS/MS scans in which the five most abundant molecular ions were dynamically selected for collision-induced dissociation using normalized collision energy of 35%. Tandem mass spectra were searched against the UniProt human proteomic database from the European Bioinformatics Institute (http://www.ebi.ac.uk/integr8) using SEQUEST (ThermoElectron). The fully tryptic peptides that have SEQUEST cross correlation scores >2.0 (+1), 2.5 (+2), or 3.0 (+3) and ΔC_n values >0.1 were considered legitimate identifications.

Recombinant expression and in vitro binding assay of ezrin and ZAP-70
ZAP-70 was subcloned into pFastBac HTb vector and transformed into Sf9 cells. Protein expression was performed according to the manufacturer's instructions (Invitrogen). Ezrin was expressed in the *Escherichia coli* strain M15 (Reczek et al., 1997). Recombinant ZAP-70 was purified and immobilized on nickel beads as previously described (Bretscher, 1983), and recombinant ezrin was purified as previously described (Reczek et al., 1997). For in vitro binding assay, similar amounts of ZAP-70 and ezrin recombinant proteins were mixed in cold buffer (50 mM Tris, pH 7.4, 100 mM NaCl, and 1 mM DTT) and incubated for 2 h with constant rotating. Beads were washed six times with the aforementioned buffer, and pellets were resuspended in SDS sample buffer, boiled, and resolved on 7.5% SDS-PAGE.

siRNA transfection
2.5×10^6 Jurkat T cells were electroporated once at 300 V and 700 μF using the Xcell Gene Pulser (Bio-Rad Laboratories) in the presence of 100 nM ezrin-specific siRNA or luciferase GL2–specific siRNA. Cells were cultured for 48 h and analyzed by immunoblotting or immunofluorescence.

Online supplemental material
Fig. S1 shows ERM expression in Jurkat T cells. Fig. S2 shows ERM dephosphorylation inhibition by calyculin A. Fig. S3 shows expression of transfected proteins in Jurkat T cells by Western blotting and immunofluorescence. Fig. S4 shows ERM protein localization in primary human T cells. Fig. S5 shows immunoprecipitation of ZAP-70 from Jurkat T cells. Online supplemental material is available at http://www.jcb.org/cgi/content/full/jcb.200707199/DC1.

We are grateful to Dr. Julie A.I. Thoms for helpful advice and for supplying the ezrin constructs. We thank Dr. A.C. Chan for providing the ZAP-70 construct.

T. Ilani was supported, in part, by a long-term European Molecular Biology Organization Fellowship. This work was supported by a National Institutes of Health grant to A. Bretscher. This project has been funded in whole or in part with federal funds from the National Cancer Institute (National Institutes of Health) under contract NO1-CO-12400.

Submitted: 27 July 2007
Accepted: 24 October 2007

References

Allenspach, E.J., P. Cullinan, J. Tong, Q. Tang, A.G. Tesciuba, J.L. Cannon, S.M. Takahashi, R. Morgan, J.K. Burkhardt, and A.I. Sperling. 2001. ERM-dependent movement of CD43 defines a novel protein complex distal to the immunological synapse. *Immunity*. 15:739–750.

Amieva, M.R., K.K. Wilgenbus, and H. Furthmayr. 1994. Radixin is a component of hepatocyte microvilli in situ. *Exp. Cell Res.* 210:140–144.

Berryman, M., Z. Franck, and A. Bretscher. 1993. Ezrin is concentrated in the apical microvilli of a wide variety of epithelial cells whereas moesin is found primarily in endothelial cells. *J. Cell Sci.* 105:1025–1043.

Boncristiano, M., M.B. Majolini, M.M. D'Elios, S. Pacini, S. Valensin, C. Ulivieri, A. Amedei, B. Falini, G. Del Prete, J.L. Telford, and C.T. Baldari. 2000. Defective recruitment and activation of ZAP-70 in common variable immunodeficiency patients with T cell defects. *Eur. J. Immunol.* 30:2632–2638.

Bretscher, A. 1983. Purification of an 80,000-dalton protein that is a component of the isolated microvillus cytoskeleton, and its localization in nonmuscle cells. *J. Cell Biol.* 97:425–432.

Bretscher, A. 1989. Rapid phosphorylation and reorganization of ezrin and spectrin accompany morphological changes induced in A-431 cells by epidermal growth factor. *J. Cell Biol.* 108:921–930.

Bretscher, A., K. Edwards, and R.G. Fehon. 2002. ERM proteins and merlin: integrators at the cell cortex. *Nat. Rev. Mol. Cell Biol.* 3:586–599.

Brown, M.J., R. Nijhara, J.A. Hallam, M. Gignac, K.M. Yamada, S.L. Erlandsen, J. Delon, M. Kruhlak, and S. Shaw. 2003. Chemokine stimulation of human peripheral blood T lymphocytes induces rapid dephosphorylation of ERM proteins, which facilitates loss of microvilli and polarization. *Blood*. 102:3890–3899.

Bunnell, S.C., D.I. Hong, J.R. Kardon, T. Yamazaki, C.J. McGlade, V.A. Barr, and L.E. Samelson. 2002. T cell receptor ligation induces the formation of dynamically regulated signaling assemblies. *J. Cell Biol.* 158:1263–1275.

Campi, G., R. Varma, and M.L. Dustin. 2005. Actin and agonist MHC-peptide complex-dependent T cell receptor microclusters as scaffolds for signaling. *J. Exp. Med.* 202:1031–1036.

Chan, A.C., M. Iwashima, C.W. Turck, and A. Weiss. 1992. ZAP-70: a 70 kd protein-tyrosine kinase that associates with the TCR zeta chain. *Cell*. 71:649–662.

Chan, A.C., T.A. Kadlecek, M.E. Elder, A.H. Filipovich, W.L. Kuo, M. Iwashima, T.G. Parslow, and A. Weiss. 1994. ZAP-70 deficiency in an autosomal recessive form of severe combined immunodeficiency. *Science*. 264:1599–1601.

Cyster, J.G., and A.F. Williams. 1992. The importance of cross-linking in the homotypic aggregation of lymphocytes induced by anti-leukosialin (CD43) antibodies. *Eur. J. Immunol.* 22:2565–2572.

Das, V., B. Nal, A. Roumier, V. Meas-Yedid, C. Zimmer, J.C. Olivo-Marin, P. Roux, P. Ferrier, A. Dautry-Varsat, and A. Alcover. 2002. Membrane-cytoskeleton interactions during the formation of the immunological synapse and subsequent T-cell activation. *Immunol. Rev.* 189:123–135.

Delon, J., K. Kaibuchi, and R.N. Germain. 2001. Exclusion of CD43 from the immunological synapse is mediated by phosphorylation-regulated relocation of the cytoskeletal adaptor moesin. *Immunity*. 15:691–701.

Doi, Y., M. Itoh, S. Yonemura, S. Ishihara, H. Takano, T. Noda, and S. Tsukita. 1999. Normal development of mice and unimpaired cell adhesion/cell motility/actin-based cytoskeleton without compensatory up-regulation of ezrin or radixin in moesin gene knockout. *J. Biol. Chem.* 274:2315–2321.

Dustin, M.L., and J.A. Cooper. 2000. The immunological synapse and the actin cytoskeleton: molecular hardware for T cell signaling. *Nat. Immunol.* 1:23–29.

Dustin, M.L., and T.A. Springer. 1988. Lymphocyte function-associated antigen-1 (LFA-1) interaction with intercellular adhesion molecule-1 (ICAM-1) is one of at least three mechanisms for lymphocyte adhesion to cultured endothelial cells. *J. Cell Biol.* 107:321–331.

Fievet, B.T., A. Gautreau, C. Roy, L. Del Maestro, P. Mangeat, D. Louvard, and M. Arpin. 2004. Phosphoinositide binding and phosphorylation act sequentially in the activation mechanism of ezrin. *J. Cell Biol.* 164:653–659.

Funayama, N., A. Nagafuchi, N. Sato, and S. Tsukita. 1991. Radixin is a novel member of the band 4.1 family. *J. Cell Biol.* 115:1039–1048.

Gary, R., and A. Bretscher. 1995. Ezrin self-association involves binding of an N-terminal domain to a normally masked C-terminal domain that includes the F-actin binding site. *Mol. Biol. Cell*. 6:1061–1075.

Gobel, V., P.L. Barrett, D.H. Hall, and J.T. Fleming. 2004. Lumen morphogenesis in *C. elegans* requires the membrane-cytoskeleton linker erm-1. *Dev. Cell*. 6:865–873.

Hirao, M., N. Sato, T. Kondo, S. Yonemura, M. Monden, T. Sasaki, Y. Takai, and S. Tsukita. 1996. Regulation mechanism of ERM (ezrin/radixin/moesin) protein/plasma membrane association: possible involvement of phosphatidylinositol turnover and Rho-dependent signaling pathway. *J. Cell Biol.* 135:37–51.

Huby, R.D., M. Iwashima, A. Weiss, and S.C. Ley. 1997. ZAP-70 protein tyrosine kinase is constitutively targeted to the T cell cortex independently of its SH2 domains. *J. Cell Biol.* 137:1639–1649.

Kikuchi, S., M. Hata, K. Fukumoto, Y. Yamane, T. Matsui, A. Tamura, S. Yonemura, H. Yamagishi, D. Keppler, and S. Tsukita. 2002. Radixin deficiency causes conjugated hyperbilirubinemia with loss of Mrp2 from bile canalicular membranes. *Nat. Genet.* 31:320–325.

Kitajiri, S., K. Fukumoto, M. Hata, H. Sasaki, T. Katsuno, T. Nakagawa, J. Ito, and S. Tsukita. 2004. Radixin deficiency causes deafness associated with progressive degeneration of cochlear stereocilia. *J. Cell Biol.* 166:559–570.

Krawczyk, C., K. Bachmaier, T. Sasaki, R.G. Jones, S.B. Snapper, D. Bouchard, I. Kozieradzki, P.S. Ohashi, F.W. Alt, and J.M. Penninger. 2000. Cbl-b is a negative regulator of receptor clustering and raft aggregation in T cells. *Immunity*. 13:463–473.

Kuhne, M.R., J. Lin, D. Yablonski, M.N. Mollenauer, L.I. Ehrlich, J. Huppa, M.M. Davis, and A. Weiss. 2003. Linker for activation of T cells, zeta-associated protein-70, and Src homology 2 domain-containing leukocyte protein-76 are required for TCR-induced microtubule-organizing center polarization. *J. Immunol.* 171:860–866.

Lankes, W.T., and H. Furthmayr. 1991. Moesin: a member of the protein 4.1-talin-ezrin family of proteins. *Proc. Natl. Acad. Sci. USA*. 88:8297–8301.

Li, Q., M.R. Nance, R. Kulikauskas, K. Nyberg, R. Fehon, P.A. Karplus, A. Bretscher, and J.J. Tesmer. 2007. Self-masking in an intact ERM-merlin protein: an active role for the central alpha-helical domain. *J. Mol. Biol.* 365:1446–1459.

Matsui, T., M. Maeda, Y. Doi, S. Yonemura, M. Amano, K. Kaibuchi, and S. Tsukita. 1998. Rho-kinase phosphorylates COOH-terminal threonines of ezrin/radixin/moesin (ERM) proteins and regulates their head-to-tail association. *J. Cell Biol.* 140:647–657.

Niedergang, F., A. Dautry-Varsat, and A. Alcover. 1997. Peptide antigen or superantigen-induced down-regulation of TCRs involves both stimulated and unstimulated receptors. *J. Immunol.* 159:1703–1710.

Nirula, A., M. Ho, H. Phee, J. Roose, and A. Weiss. 2006. Phosphoinositide-dependent kinase 1 targets protein kinase A in a pathway that regulates interleukin 4. *J. Exp. Med.* 203:1733–1744.

Pearson, M.A., D. Reczek, A. Bretscher, and P.A. Karplus. 2000. Structure of the ERM protein moesin reveals the FERM domain fold masked by an extended actin binding tail domain. *Cell*. 101:259–270.

Reczek, D., M. Berryman, and A. Bretscher. 1997. Identification of EBP50: A PDZ-containing phosphoprotein that associates with members of the ezrin-radixin-moesin family. *J. Cell Biol.* 139:169–179.

Saotome, I., M. Curto, and A.I. McClatchey. 2004. Ezrin is essential for epithelial organization and villus morphogenesis in the developing intestine. *Dev. Cell*. 6:855–864.

Sasahara, Y., R. Rachid, M.J. Byrne, M.A. de la Fuente, R.T. Abraham, N. Ramesh, and R.S. Geha. 2002. Mechanism of recruitment of WASP to the immunological synapse and of its activation following TCR ligation. *Mol. Cell*. 10:1269–1281.

Sato, N., N. Funayama, A. Nagafuchi, S. Yonemura, and S. Tsukita. 1992. A gene family consisting of ezrin, radixin and moesin. Its specific localization at actin filament/plasma membrane association sites. *J. Cell Sci.* 103:131–143.

Serrador, J.M., M. Nieto, J.L. Alonso-Lebrero, M.A. del Pozo, J. Calvo, H. Furthmayr, R. Schwartz-Albiez, F. Lozano, R. Gonzalez-Amaro, P. Sanchez-Mateos, and F. Sanchez-Madrid. 1998. CD43 interacts with moesin and ezrin and regulates its redistribution to the uropods of T lymphocytes at the cell-cell contacts. *Blood*. 91:4632–4644.

Shaw, A.S. 2001. FERMing up the synapse. *Immunity*. 15:683–686.

Shcherbina, A., A. Bretscher, D.M. Kenney, and E. Remold-O'Donnell. 1999. Moesin, the major ERM protein of lymphocytes and platelets, differs from ezrin in its insensitivity to calpain. *FEBS Lett.* 443:31–36.

Speck, O., S.C. Hughes, N.K. Noren, R.M. Kulikauskas, and R.G. Fehon. 2003. Moesin functions antagonistically to the Rho pathway to maintain epithelial integrity. *Nature*. 421:83–87.

Takeuchi, K., N. Sato, H. Kasahara, N. Funayama, A. Nagafuchi, S. Yonemura, and S. Tsukita. 1994. Perturbation of cell adhesion and microvilli formation by antisense oligonucleotides to ERM family members. *J. Cell Biol.* 125:1371–1384.

Tskvitaria-Fuller, I., A.L. Rozelle, H.L. Yin, and C. Wulfing. 2003. Regulation of sustained actin dynamics by the TCR and costimulation as a mechanism of receptor localization. *J. Immunol.* 171:2287–2295.

Tsukita, S., and Y. Hieda. 1989. A new 82-kD barbed end-capping protein (radixin) localized in the cell-to-cell adherens junction: purification and characterization. *J. Cell Biol.* 108:2369–2382.

Turunen, O., T. Wahlstrom, and A. Vaheri. 1994. Ezrin has a COOH-terminal actin-binding site that is conserved in the ezrin protein family. *J. Cell Biol.* 126:1445–1453.

Urzainqui, A., J.M. Serrador, F. Viedma, M. Yanez-Mo, A. Rodriguez, A.L. Corbi, J.L. Alonso-Lebrero, A. Luque, M. Deckert, J. Vazquez, and F. Sanchez-Madrid. 2002. ITAM-based interaction of ERM proteins with Syk mediates signaling by the leukocyte adhesion receptor PSGL-1. *Immunity*. 17:401–412.

Vicente-Manzanares, M., and F. Sanchez-Madrid. 2004. Role of the cytoskeleton during leukocyte responses. *Nat. Rev. Immunol.* 4:110–122.

Williams, B.L., B.J. Irvin, S.L. Sutor, C.C. Chini, E. Yacyshyn, J. Bubeck Wardenburg, M. Dalton, A.C. Chan, and R.T. Abraham. 1999. Phosphorylation of Tyr319 in ZAP-70 is required for T-cell antigen receptor-dependent phospholipase C-gamma1 and Ras activation. *EMBO J.* 18:1832–1844.

Yang, H.S., and P.W. Hinds. 2003. Increased ezrin expression and activation by CDK5 coincident with acquisition of the senescent phenotype. *Mol. Cell*. 11:1163–1176.

Yokosuka, T., K. Sakata-Sogawa, W. Kobayashi, M. Hiroshima, A. Hashimoto-Tane, M. Tokunaga, M.L. Dustin, and T. Saito. 2005. Newly generated T cell receptor microclusters initiate and sustain T cell activation by recruitment of Zap70 and SLP-76. *Nat. Immunol.* 6:1253–1262.

Yonemura, S., M. Hirao, Y. Doi, N. Takahashi, T. Kondo, and S. Tsukita. 1998. Ezrin/radixin/moesin (ERM) proteins bind to a positively charged amino acid cluster in the juxta-membrane cytoplasmic domain of CD44, CD43, and ICAM-2. *J. Cell Biol.* 140:885–895.